Eur Biophys J (2009) 38:229–235
DOI 10.1007/s00249-008-0374-0

ORIGINAL PAPER

Structural organisation of cationic dioctadecyldimethyammonium bromide monolayers in presence of hyaluronic acid

R. Ionov · A. El-Abed · M. Goldmann

Received: 7 July 2008 / Revised: 21 September 2008 / Accepted: 22 September 2008 / Published online: 7 October 2008

Abstract Langmuir monolayers of dioctadecyldimethyammonium bromide and its interaction with the natural mucopolysaccharide hyaluronic acid are studied using thermodynamic methods and X-ray diffraction at grazing incidence. The 2D crystalline lattice parameters of different phases are determined. The monolayer compressibility, the linear crystalline compressibility components and the thermoelastic expansion coefficient are evaluated. The biopolymer stabilises the monolayer structural properties, increases the collapse pressure and the correlation length of the 2D crystalline domains. The results show that this lipid has a potential for developing of stabilised drug delivery systems of anionic biopolymers like hyaluronic acid, oligomers and genes.

R. Ionov · A. El-Abed
LNPC, Université René Descartes,
45, rue des Saints Pères, 75270 Paris Cedex 06, France

R. Ionov
College of Sciences Leonardo da Vinci,
PO Box 946, 1000 Sofia, Bulgaria

M. Goldmann
Institut des Nano-Sciences de Paris,
UMR-CNRS 7588, Universités de Paris 6 et 7,
140 rue de Lourmel, 75015 Paris, France

M. Goldmann
LURE, Université Paris Sud, 91405 Orsay, France

R. Ionov (✉)
6 Cité d'Angouleme, 75011 Paris, France
e-mail: r_ionov@hotmail.com

Keywords Model membranes · Langmuir monolayers · Hyaluronic acid · Cationic lipids · 2D crystals · Drug delivery

Introduction

Cationic lipids are of major interest as drug delivery systems of negatively charged drugs, proteins, biopolymers, genes and vaccines (Olsen et al. 2001; Vangala et al. 2007; Brishall et al. 1999). They can be formulated as liposomes or as nano-objects (Rosenecker et al. 1996; Ahmed et al. 2002; Li et al. 2006; Zeisig et al. 1998; Scholer et al. 2002). Dioctadecyldimethyammonium bromide (DODAB, Fig. 1a) is an interesting cationic lipid with both lamellar and nonlamellar properties that can form different bilayers or monolayer systems (Rosenecker et al. 1996; Ahmed et al. 2002; Li et al. 2006; Zeisig et al. 1998; Scholer et al. 2002; Ionov and Angelova 1996; Wang et al. 2006; Gouard et al. 2007; Engelking et al. 1999). Charged lipid interfaces are relevant to the biological membranes, where the charged lipids may appear because of the lipid metabolism.

In our previous study (Ionov et al. 2004a, b), we have shown that the electrostatic, hydrogen and van der Waals interactions at the membrane interface can dramatically change its properties. The state of the membrane depends on the physico-chemical characteristics of both the lipids and the membrane-bound proteins. Negatively charged biopolymers like hyaluronic acid are able to induce structural reorganisation of cationic lipid monolayers.

Hyaluronic acid (Fig. 1a) is a natural high molecular weight unbranched polysaccharide found throughout connective tissues. In some tissues, like vitreous humour, synovial fluid, it is the primary component responsible for the function and the physical characteristics associated

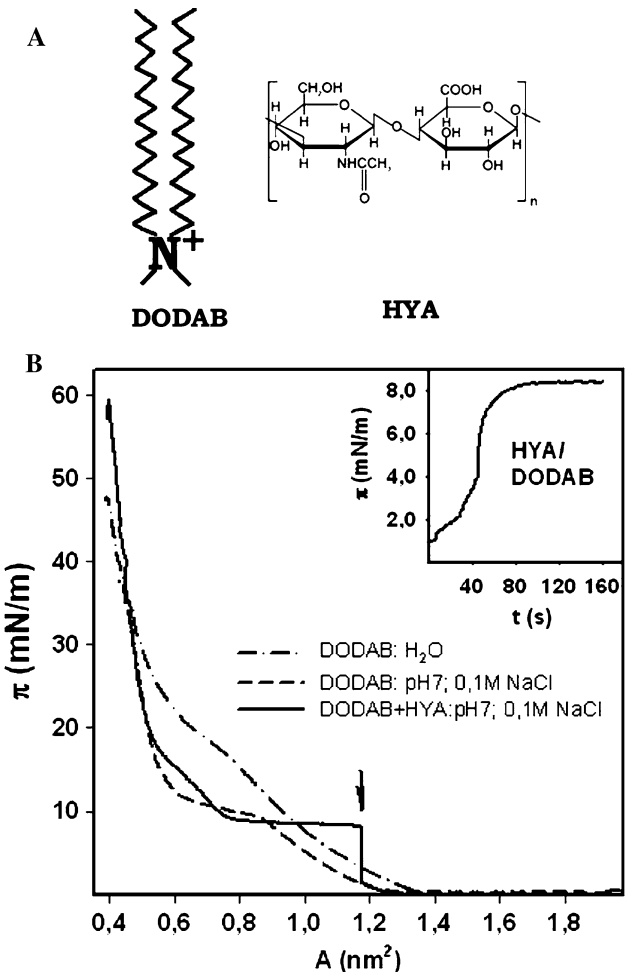

Fig. 1 **a** Structure of DODAB and HYA. **b** Langmuir monolayer isotherms of DODAB and DODAB + HYA at 20°C and different subphases. The *arrow* indicates the injection of HYA under DODAB monolayer. The *inset* shows adsorption kinetics of HYA under DODAB monolayer

with these substances (Dea et al. 1973; Flowers et al. 1992; Shard et al. 1997; Arnott et al. 1983). In other tissues such as skin, cartilage and aorta it is found as a minority component which acts as a stabilising and organising agent on the structure of some proteins (Dea et al. 1973). Hyaluronic acid (HYA) and its derivatives are broadly used in pharmacy and medicine, especially in segment surgery, wound and burn therapy, drug matrices, HIV-antibody (Hume et al. 1994; Zheng et al. 1994; Ruiz-Cardona et al. 1996; Joshi and Topp 1992). Many of the functions of the hyaluronic acid are related to its physico-chemical and structural properties as well as to its interactions with membrane lipids (Sung and Topp 1995; Artzner et al. 2000; Ruponena et al. 1999; Nitzan et al. 2001; Herslof-Bjorling et al. 1996). For example, the vitreous humour is constituted of 99% water and 1% mixture of collagen and hyaluronic acid. HYA is an active pH dependent biopolymer, which may influence the state of the neighbour Burch membrane. In concentrated solutions, due to the hydrogen bonds, various conformations of this mucopolysaccharide are probable; from double helices to compact states of densely packed chains (Dea et al. 1973; Atkins and Sheehan 1973; Lee et al. 1992; Mitra et al. 1983; Sheehan and Atkins 1983; Sheehan et al. 1975). At the charged lipid interface, its structure differs from the bulk state (Ionov et al. 2004a, b).

Our previous study (Ionov et al. 2004a, b) showed that HYA interacted actively with single chain octadecylammonium cationic monolayers, stabilised and reorganised them. In this study, we use DODAB that forms Langmuir monolayers at the air/water interface of higher stability due to its double chain structure. Langmuir monolayers are suitable systems to study the interactions at the membrane interface (Ionov et al. 2000; Petty 1996; Nakazawa et al. 2004; Patino and Fernandezs 2004; Loste et al. 2003; Ionov and Angelova 1995; Ionov et al. 2004a, b; El Abed et al. 2001). We investigate the role of electrostatic interactions and the effects induced by hyaluronic acid on DODAB monolayer organisation as well as the adsorption kinetics by using thermodynamical and structural approaches.

Materials and methods

Dioctadecyldimethyammonium bromide (DODAB) and hyaluronic acid (HYA) sodium salt from bovine tracheae were Fluka products. HYA mean molecular weight was of about 80,000 Da. The salts and solvents were high purity Merck, Fluka, Prolabo, and Sigma products. The physiological aqueous solution contained 0.1 M NaCl of pH 7.0, which was adjusted by means of 1.10^{-3} M phosphate buffer (Na_2HPO_4/NaH_2PO_4 of 1/1 molar ratio, p.a. grade, Merck). Deionised pure water of resistivity 1.8×10^7 Ω cm was used (ELGA filter system). The temperature of the subphase was controlled with precision of 0.1°C.

The adsorption was performed by injection of 10^{-3} M water solutions of hyaluronic acid under the pure air/water interface or under lipid/water interface.

An automatically controlled Langmuir trough (Ionov et al. 2004a, b, 2000) was used to study the lipid monolayers. Surface pressure was measured by means of the Wilhelmy plate method with precision of about 0.1 mN m^{-1}. The monolayer compression speed was about 0.01 nm^2 per molecule per min. The temperature region of the trough operation was from 0 to 70°C. DODAB chloroform solutions of 1×10^{-3} M were used. A chloroform evaporation period of 1,800 s was allowed prior to compression of monolayers.

The 2D monolayer isothermal compressibility was determined by using linear fitting procedure for corresponding liquid expanded–liquid condensed LE and LC phase regions of stable DODAB monolayers at physiological

conditions (0.1 M NaCl of pH 7.0) and in presence of HYA. At pure water subphase, the monolayer instability does not allow to obtain reproducible compressibility values.

Synchrotron X-ray diffraction experiments from lipid monolayers were performed at LURE, Orsay, France using the experimental equipment (Fontaine et al. 2004) at the beam line D41B.

The adsorption kinetics was analysed using non-linear least square fit procedure of the Origin software (Microcal. Inc. USA).

Results

The surface pressure/area isotherms of the cationic DODAB Langmuir monolayers at 20°C are shown on Fig. 1. The collapse pressure is at 48 mN m^{-1}. The surface area at 35 mN m^{-1} is 0.53 nm^2. At physiological conditions (0.1 M NaCl of pH 7.0), the monolayers show clear transition region from 0.9 to 0.6 nm^2 with slight surface pressure rise from 8.5 to 11.5 mN m^{-1}. This region is more smeared at pure water subphase with steeper rise of surface pressure from 10 to 22 mN m^{-1}. At pure water subphase the isotherm is not very stable: for example the surface area at 35 mN m^{-1} decreased with 0.04 nm^2 for a time period of 900 s. Monolayer equilibrium surface pressure (ESP) is determined to be 42.5 mN m^{-1}.

Hyaluronic acid volume concentration of 1×10^{-6} M was injected in the subphase under the lipid monolayer compressed to about 1 mN m^{-1} at physiological conditions. Due to the surface activity of hyaluronic acid, the pressure rises to hyaluronic acid ESP steady state value of about 8.2 mN m^{-1}. Thereafter, the film was compressed. The isotherms at higher surface pressure values coincide with those of the pure DODAB monolayers in absence of hyaluronic acid. The DODAB monolayers are stable in presence of HYA in the subphase and the collapse pressure rises to about 58 mN m^{-1}.

The adsorption kinetics of HYA under DODAB is a fast one-step process with relaxation time of 46 s (Fig. 1, inset).

Grazing incidence X-ray diffraction (GIXD) patterns were detected from the monolayers in the LC regions above 18 mN m^{-1}. Figure 2a shows DODAB monolayer X-ray diffraction patterns obtained at 35 mN m^{-1} and physiological conditions at air/water interface. The three peaks at 1.204 (very diffuse); 1.346 and 1.406 $Å^{-1}$ in Q vector space are assigned to Q_{11}, Q_{01} and Q_{10} components, respectively. They are Lorenz peaks with full widths at half maximum (FWHM) of 0.034, 0.036 and 0.042 $Å^{-1}$, respectively. Rod scans on Fig. 2b show that these peaks are planar. Similar types of rod scans are obtained from all monolayers in this study.

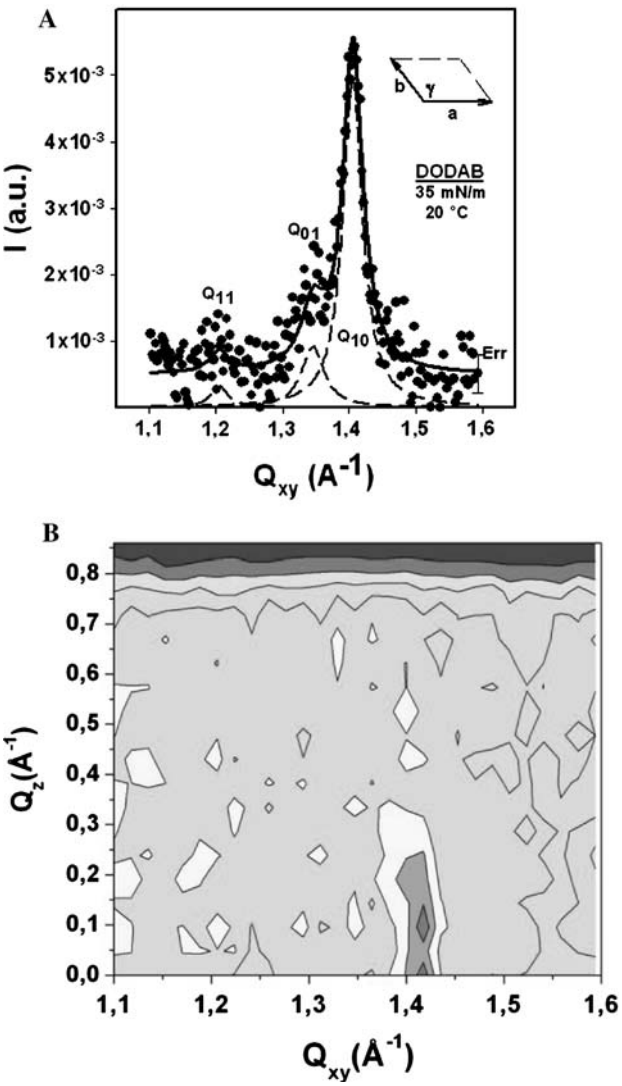

Fig. 2 **a** GIXD patterns of DODAB monolayer compressed to 35 mN m^{-1} at 20°C and at physiological conditions (0.1 M NaCl of pH 7.0). The spectrum is decomposed on three Lorenz peaks. *Err* indicate the error bars. The oblique lattice is indicated on the *inset*. **b** Rod scans are presented as contour plots of Q_z as a function of the planar wavevector Q_{xy}

Figure 3 presents the variation of the diffraction patterns with the surface pressure for both DODAB and DODAB + HYA monolayers at room temperature of 20°C. The inset shows the variation of the main peak Q_{10}. DODAB peak follows a linear dependence, while the peak position in presence of HYA is approximately constant in the limits of the experimental error.

The temperature dependence of the diffraction patterns at 35 mN m^{-1} are shown on Fig. 4. The peak intensity increases and FWHM narrows for DODAB monolayers, while they remain unchanged for DODAB + HYA monolayers with decreasing the temperature. Q_{10} peak position follows approximately the same linear dependence for both

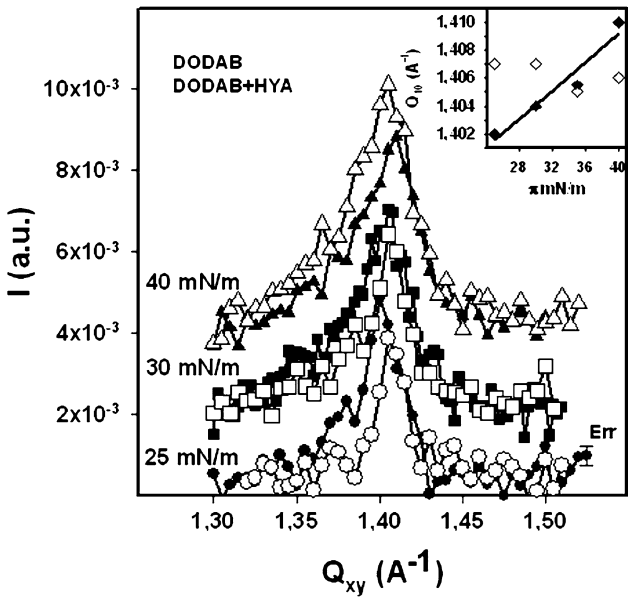

Fig. 3 GIXD patterns of DODAB and DODAB + HYA monolayers as a function of the surface pressure at 20°C and physiological conditions (0.1 M NaCl of pH 7.0). The *open symbols* are DODAB + HYA data. *Err* indicate the error bars. The *inset* shows the surface pressure dependence of the strongest wavevector component

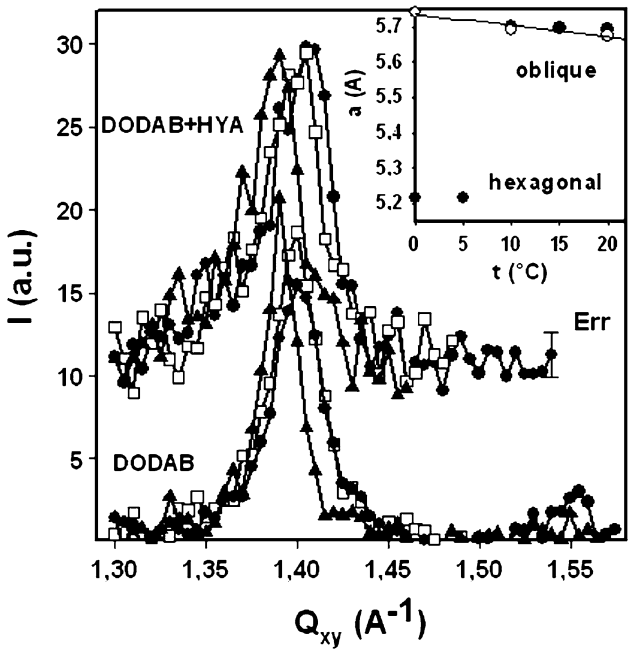

Fig. 4 Temperature GIXD patterns variation of DODAB and DODAB + HYA monolayers at 35 mN m^{-1} at physiological conditions (0.1 M NaCl of pH 7.0). *Circles* 20°C, *open squares* 10°C and *triangles* −0°C. *Err* indicate the error bars. The *inset* shows a lattice temperature variation of oblique and hexagonal structures. The *open symbols* are DODAB + HYA data

monolayers (Fig. 4, inset). A single Lorenz DODAB monolayer peak at about $Q_{10} = 1.390$ $Å^{-1}$ is detected for temperatures below 10°C.

Discussion

DODAB isotherm (Fig. 1) presents a liquid expanded-liquid condensed (LE–LC) phase transition region. This region is better expressed at physiological condition (0.1 M NaCl of pH 7.0) in comparison to pure water subphase. It is well known that the electrostatic interactions between 2D domains cause variations of the slope of the plateau region that may explain the difference of the pure water and physiological condition monolayer isotherms. Surface potential isotherm analysis based on Gouy Chapman theory shows that the effective surface charge density of DODAB monolayers increases with the electro-negativity of the counterions in the subphase (Cavali et al. 2001; Dynarowicz-Latka et al. 2001; Taylor et al. 1989). The pressure area isotherms change from condensed to expanded monolayer with the increase of the surface charge density and corresponding electrostatic repulsion between head groups. In the framework of this analysis, the presence of HYA reduces the effective surface charge density of DODAB monolayers and the isotherms become more condensed.

Monolayer isotherm may depend on the presence of solvent traces as well. For a good solvent like chloroform used in our experiments, a minimum evaporation time of about 900 s should be allowed. Our waiting time was doubled to avoid this problem. Our DODAB monolayer isotherms at pure water subphase fit to the literature data (Wang et al. 2006; Gouard et al. 2007). DODAB molecular areas reported at pure water subphase vary from 0.50 to 0.66 nm^2 and are higher than the area of about 0.44 nm^2 of two aliphatic chains. The area differences originate from monolayer instability at pure water subphase. Participation of water molecules in lateral DODAB structural organisation may be speculated as well.

DODAB monolayer instability at pure water surface arises from the DODAB intramolecular misbalance of hydrophobic and hydrophilic interactions. The head group cation that is favourable to water hydration is buried in a hydrophobic-like methyl shell that has an opposite tendency to repel the water. This reduces the strength of head group–aqueous subphase interactions, results in misbalance of the hydrophobic/hydrophilic distribution of the lateral intralayer pressure and correspondingly increases the monolayer instability. Upon compression, the molecules have the tendency to escape in the 3D air region due to the misbalance induced vertical force component. The phenomenon is similar to the head group misbalance shape origin of

nonlamellar lipid phases like in dioleolylphosphatidylethanolamine (DOPE). However, DOPE monolayers show good surface stability (Ionov et al. 2000) due to the presence of additional hydrophilic intramolecular phosphate buffer in the head group region that increases the head group hydrophilic interactions with the aqueous subphase.

The introduction of additional electrostatic interactions with the aqueous subphase at physiological conditions results in better DODAB monolayer stability. The electrostatic interactions of the cationic DODAB monolayer and the negatively charged biopolymer HYA prevent the DODAB molecules to escape in 3D phase, stabilise the monolayer isotherm and the collapse surface pressure rises to a higher value. This stabilisation is without other noticeable structural reorganisation that influences the monolayer isotherm. Such more pronounced monolayer stabilisation effect was observed for single chain octadecylamine monolayers in our previous study (Ionov et al. 2004a, b). DODAB monolayer properties are influenced by the stronger double chain van der Waals lateral interactions and are more stable in respect to octadecylammonium monolayers. The molecular area of 0.53 nm^2 determined at physiological conditions is higher than the area of two aliphatic chains. Having in mind the water structural data (O–H bond length of 0.096 nm, HOH angle of 104.45° and hydrogen bond length of 0.197 nm), one may speculate that between 1 and 2 water molecules participate in the lateral structural organisation of DODAB monolayer. This may explain the origin of the negative thermoelastic linear expansion coefficients reported below.

The 2D monolayer isothermal compressibility

$$\beta = -\frac{1}{A}\left(\frac{\partial A}{\partial \pi}\right)_T \quad (1)$$

(where, A is the molecular area and π is the surface pressure) of LE and of LC phase regions are 36.7 and 8.7 m N^{-1} respectively. They are determined for stable monolayers in presence of HYA and at physiological conditions. These values are typical for LE and LC phase regions reported in the literature for amphiphilic monolayers (Petty 1996; Ionov et al. 2000). In LE phase, the lipid chains are in fluid-like expanded state that results in higher compressibility. The small compressibility of LC phase indicates that the lipid chains are organised in 2D crystalline state.

The adsorption kinetics of HYA under DODAB is a fast one-step process (Fig. 1, inset). It could be described in terms of first order equation (Jones and Chapman 1995).

$$\pi_t = \pi_s - (\pi_s - \pi_0)e^{-\frac{t}{\tau}} \quad (2)$$

where τ is the relaxation time, π_0, π_t and π_s are the surface pressures at time $t = 0$, t and steady state conditions. This process is determined by the balance between the adsorption/desorption events, molecular rearrangements and structuration at the interface. At low concentrations of HYA, the role of desorption is important. At higher concentrations, the desorption flux is lower because of higher probability of hydrogen bond formation and molecular reorganisation. The fast relaxation time of 46 s of HYA under DODAB monolayer is related to reduced role of the desorption process due to the electrostatic interactions between the positively charged monolayer and the negatively charged biopolymer. The relaxation process differs from the two-step process observed previously with octadecylammonium monolayers (Ionov et al. 2004a, b). The second octadecylammonium monolayer reorganisation step is not observed with DODAB-HYA monolayer. This could be due to higher monolayer stability because of stronger lateral van der Waals interactions between double chained molecules.

GIXD results of DODAB monolayers on Fig. 2a permit to determine an oblique 2D unit crystalline lattice with parameters $a = 5.683 \pm 0.002$ Å; $b = 5.931 \pm 0.002$ Å and $\gamma = 128°$ for aliphatic chains of the chiral LC phase. The scheme of the unit cell is shown in the inset in Fig. 2a. The molecular area determined from these parameters fits to area of 0.53 nm^2 determined from monolayer isotherm. Two-dimensional crystalline domains have a correlation length of about 60 Å calculated from the peak FWHM. The rod scans (Fig. 2b) show that the aliphatic chains are oriented perpendicularly to the air/water interface.

While the pure DODAB monolayer peak positions vary with the surface pressure (Fig. 3), the monolayers stabilised by HYA presents peaks that are not essentially influenced by monolayer compression. The electrostatic interactions of DODAB and HYA also contribute to higher 2D crystalline domain size. The Lorenz peaks are narrow with correlation length of about 140 Å, while for pure DODAB monolayer the correlation length is about two times shorter 60 Å. On approaching ESP values at 40 mN m^{-1} the DODAB + HYA peak position remains stable but its FWHM increases that determine a reduced correlation lengths of about 70 Å. Pure DODAB monolayers at these pressures are not very stable, they show a progressive collapse and peak intensities drop down.

The linear isothermal elastic compressibility can be related to the elastic tensor (Fradin et al. 1998). For 2D crystal, they are in general anisotropic with characteristic values β_a and β_b along the unit cell axes. 2D DODAB linear crystalline compressibilities are $\beta_a = 0.36$ and $\beta_b = 0.21$ m N^{-1}. The DODAB + HYA compressibilities are very small and fall within our experimental error. We shall notice that the compressibility determinations by GIXD and by monolayer isotherms are different. While GIXD is sensitive only to large scale 2D crystalline parameters, the monolayer isotherms depend on both the crystalline and the noncrystalline phase behaviour as well as influenced by slow collapses and 3D molecular transitions.

The electrostatic interactions of HYA and DODAB contribute to maintain the domain size unchanged with decreasing the temperature (Fig. 4). In pure DODAB monolayers, FWHM narrows at lower temperatures and correspondingly the correlation length increases from 60 to 85 Å in the temperature range between 20 and 0°C, respectively. These monolayers undergo a phase transition at about 10°C from 2D oblique to 2D hexagonal phase aliphatic chains with $a = b = 5.218 \pm 0.002$ Å and $\gamma = 120°$. The aliphatic chains remain upright as detected by rod scans (Fig. 2b).

The linear isobar thermoelastic expansion coefficient is related in general to the elastic tensor (Lifshitz et al. 1993). It is anisotropic for crystals and its linear components can be determined along the crystal axes. For the axis **a** it is determined as

$$\alpha_a = \frac{1}{a}\left(\frac{\partial a}{\partial T}\right)_p \tag{3}$$

where, a is the length along **a**, T is the temperature and p the pressure.

Our results (Fig. 4, inset) show that the oblique lattice data of both DODAB and DODAB + HYA monolayers follow linear dependence with negative linear expansion coefficients along the axis **a** $\alpha_{ad} = -1.5 \times 10^{-4}$ K^{-1} and $\alpha_{adh} = -5.7 \times 10^{-4}$ K^{-1}, respectively. It is well known that water has negative isobar thermoelastic expansion coefficient. HYA is strongly hydrated. Both, the steric and electrostatic interactions (discussed above) require the hydration of DODAB head group region to ensure monolayer stability. Monolayer areas indicate a participation of water molecules in the lateral structural organisation of DODAB monolayers. Water molecules are present in the 2D crystalline lattice and they influence the monolayer linear isobar thermoelastic expansion coefficient. These results indicate the importance of DODAB head group and HYA hydration on monolayer structural organisation.

In this work, we have studied the structural organisation of cationic DODAB monolayers and the induced effects as a result of electrostatic interactions with the negatively charged HYA biopolymer. The results show that biopolymers interact with membrane interface and they are able to stabilise and alter the membrane properties. DODAB + HYA system may be interesting for developing stable vectors of active molecules. DODAB liposomes may be useful to deliver negatively charged drugs like genes and biopolymers.

References

Ahmed K, Gribbon P, Jones M (2002) The application of confocal microscopy to the study of liposome adsorption onto bacterial biofilms. J Liposome Res 12:285–300. doi:10.1081/LPR-120016195

Arnott S, Mitra A, Raghunathan S (1983) Hyaluronic acid double helix. J Mol Biol 169:861–872. doi:10.1016/S0022-2836(83)80140-5

Artzner F, Zantl R, Rädler JO (2000) Lipid–DNA and lipid–polyelectrolyte mesophases, structure and exchange kinetics. Cell Mol Biol 46:967–978

Atkins E, Sheehan J (1973) Hyaluronates: relations between molecular conformations. Science 179:562–564. doi:10.1126/science.179.4073.562

Brishall J, Kellaway I, Mills S (1999) Physico-chemical characterisation and transfection efficiency of lipid-based gene delivery complexes. Int J Pharm 183:195–207. doi:10.1016/S0378-5173(99)00117-9

Cavali A, Dynarowicz-Latka P, Oliveira ON Jr, Feitosa E (2001) Using an effective surface charge to explain surface potentials of Langmuir monolayers from dialkyldimethylammonium halides with Gouy–Chapman theory. Chem Phys Lett 338:88–94. doi:10.1016/S0009-2614(01)00272-X

Dea I, Moorhouse R, Rees D, Arnott S, Guss J, Balazs E (1973) Hyaluronic acid: a novel, double helical molecule. Science 179:560–562. doi:10.1126/science.179.4073.560

Dynarowicz-Latka P, Dhanabalan A, Oliveira O Jr (2001) Adv Colloid Interface Sci 91:221–293. doi:10.1016/S0001-8686(99)00034-2

El Abed A, Ionov R, Goldmann M, Fontaine P, Billard J, Peretti P (2001) Evidence for asymmetric edge-on Langmuir monolayer: application to surface potential measurements. Europhys Lett 56:234–240. doi:10.1209/epl/i2001-00511-0

Engelking J, Ulbrich D, Meyer W, Schenk-Meuser K, Duschner H, Menzel H (1999) Complexes of anionic poly(*p*-phenylene) polyelectrolyte and dioctadecylammonium bromide at the air water interface. Mater Sci Eng C 8:29–34. doi:10.1016/S0928-4931(99)00051-X

Flowers M, Marlowe R, Lee S, Lavalle N, Rupprecht A (1992) Optical and physical properties of wet-spin films of Na hyaluronate. Biophys J 63:323–326

Fontaine P, Goldmann M, Bordessoule M, Jucha A (2004) Grazing incidence X-ray diffraction from Langmuir monolayers. Rev Sci Instrum 75:3097–3103. doi:10.1063/1.1790582

Fradin C, Daillant J, Braslau A, Luzet D, Alba M, Goldmann M (1998) Microscopic measurement of the linear compressibilities of two-dimensional fatty acid mesophases. Eur Phys J B 1:57–65. doi:10.1007/s100510050152

Gouard F, Fichet O, Teyssié D, Fontaine P, Goldmann M (2007) Characterisation limits of a polymer adsorbed under a monolayer by GIXD measurements. J Coll Int Sci 306:82–88. doi:10.1016/j.jcis.2006.10.016

Herslof-Bjorling A, Sunderlof L, Porch B, Valtcheva L, Hjerten S (1996) Interaction of anionic polysaccharide and an oppositely charged surfactant. Langmuir 12:4628–4637. doi:10.1021/la950222o

Hume L, Lee H, Benedetti L, Sanzgiri Y, Topp E, Stella V (1994) Ocular sustained delivery of prednisolone using hyaluronic acid benzyl ester films. Int J Pharm 111:295–298. doi:10.1016/0378-5173(94)90352-2

Ionov R, Angelova A (1995) Evidence for a discotic smectic-nematic phase induced in Langmuir–Blodgett films. Phys Rev E Stat Phys Plasmas Fluids Relat Interdiscip Topics 52:R21–R25. doi:10.1103/PhysRevE.52.R21

Ionov R, Angelova A (1996) Swelling of bilayer lipid membranes: FTIR and X-ray study. Thin Solid Films 284/285:809–812. doi:10.1016/S0040-6090(95)08452-5

Ionov R, El-Abed A, Angelova A, Goldmann M, Peretti P (2000) Assymetrical ion channel model inferred from two dimensional crystallization of peptide antibiotic. Biophys J 78:3026–3035

Ionov R, El-Abed A, Goldmann M, Peretti P (2004a) Interaction of lipid monolayers with the natural biopolymer hyaluronic acid.

Biochem Biophys Acta 1667:200–207. doi:10.1016/j.bbamem.2004.10.007

Ionov R, El-Abed A, Goldmann M, Peretti P (2004b) Structural organization of helical peptide antibiotic alamethicin at the air/water interface. J Phys Chem B 108:8485–8488. doi:10.1021/jp049271c

Jones M, Chapman D (1995) Micelles, monolayers and biomembranes. Wiley-Liss, New York

Joshi H, Topp E (1992) Hydration in hyaluronic acid and its esters using differential scanning calorimetry. Int J Pharm 80:213–225. doi:10.1016/0378-5173(92)90279-B

Lee S, Oliver W, Rupprecht A, Song Z, Lindsay S (1992) Observation of a phase transition in wet-spin films of Na hyaluronate. Biopolymers 32:303–306. doi:10.1002/bip.360320310

Li W, Li H, Wu L (2006) Structural characterisation of dimethyldioctadecylammonium-encapsulated terbium-substituted heteropolyoxotungatates in solid, Langmuir–Blodgett and solvent casting films. Colloids Surfaces A 272:176–181. doi:10.1016/j.colsurfa.2005.07.021

Lifshitz E, Landau L, Pitaevskii L (1993) Theory of elasticity, Nauka, Moscow

Loste E, Díaz-Martí E, Zarbakhsh A, Meldrum FC (2003) Study of calcium carbonate precipitation under a series of fatty acid Langmuir monolayers using Brewster angle microscopy. Langmuir 19:2830–2837

Mitra A, Raghunathan S, Sheehan J, Arnott S (1983) Hyaluronic acid: molecular conformations and interactions in the orthorhombic and tetragonal forms containing sinuous chains. J Mol Biol 169:829–859. doi:10.1016/S0022-2836(83)80139-9

Nakazawa T, Azumi R, Sakai H, Abe M, Matsumoto M (2004) Brewster angle microscopic observations of the Langmuir films of amphiphilic spiropyran during compression and under UV illumination. Langmuir 20:5439–5444. doi:10.1021/la049582e

Nitzan DW, Nitzan U, Dan P, Yedgar S (2001) The role of hyaluronic acid in protecting surface-active phospholipids from lysis by exogenous phospholipase. Rheumatology 40:336–340. doi:10.1093/rheumatology/40.3.336

Olsen A, Pinxteren L, Okkels M, Rasmussen P, Andersen P (2001) Protection of mice with a tuberculosis subunit vaccine. Infect Immun 69:2773–2778. doi:10.1128/IAI.69.5.2773-2778.2001

Patino JM, Fernandez MC (2004) Structural and topographical characteristics of adsorbed WPI and monoglyceride mixed monolayers at the air–water interface. Langmuir 20:4515–4522. doi:10.1021/la036190j

Petty M (1996) Langmuir Blodgett films—an introduction. Cambridge University Press, Cambridge

Rosenecker J, Zhang W, Hong K, Gepetti P, Youshihara S, Papahadjopoulous D, Nadel J (1996) Increased liposome extravasation at selected tissues. Proc Natl Acad Sci USA 93:7236–7241. doi:10.1073/pnas.93.14.7236

Ruiz-Cardona L, Sanzgiri Y, Benedetti L, Stella V, Topp E (1996) Application of benzyl hyaluronate membranes as potential wound dressing: evaluation of water vapour and gas permeabilities. Biomaterials 17:1639–1643. doi:10.1016/0142-9612(95)00324-X

Ruponena M, Ylä-Herttualab S, Urttia A (1999) Interactions of polymeric and lyposomal gene delivery systems with extracellular glycosaminoglycans: physicochemical and transfection studies. Biochim Biophys Acta 1415:331–341. doi:10.1016/S0005-2736(98)00199-0

Scholer N, Hahn H, Muller R, Liesenfeld O (2002) Effect of lipid matrix and size of solid lipid nanoparticles on the viability and cytokine production of macrophages. Int J Pharm 231:167–176. doi:10.1016/S0378-5173(01)00882-1

Shard A, Davies M, Tendler S, Benedetti L, Purbrick M, Paul A, Beamson G (1997) X-ray photoelectron spectroscopy and time of flight SIMS investigations of hyaluronic acid derivatives. Langmuir 13:2808–2814. doi:10.1021/la960050a

Sheehan J, Atkins E (1983) X-ray fibre diffraction study of conformational changes in hyaluronate induced in presence of sodium, potassium and calcium cations. Int J Biol Macromol 5:215–221. doi:10.1016/0141-8130(83)90005-3

Sheehan J, Atkins E, Nieduszynski I (1975) X-ray diffraction study on the connective tissue polysaccharides. J Mol Biol 91:153–163. doi:10.1016/0022-2836(75)90156-4

Sung K, Topp E (1995) Effect of drug hydrophilicity and membrane hydration on diffusion in hyaluronic acid ester membranes. J Control Release 37:95–104. doi:10.1016/0168-3659(95)00068-J

Taylor D, Oliveira ON Jr, Morgan H (1989) Stearic acid monolayers. Chem Phys Lett 161:147–153. doi:10.1016/0009-2614(89)85047-X

Vangala A, Bramwell W, McNeil S, Christensen D, Agger E, Perrie Y (2007) Comparison of vesicle based antigen delivery systems for delivery of hepatitis B surface antigen. J Control Release 119:102–110. doi:10.1016/j.jconrel.2007.01.010

Wang Y, Pereira C, Marques E, Brito R, Fereira E, Silva F (2006) Cationic surfactants at the air/water interface. Thin Solid Films 515:2031–2037. doi:10.1016/j.tsf.2006.04.044

Zeisig R, Arndt D, Stahn R, Fishtner I (1998) Physical properties and pharmacological activity in vitro and in vivo of optimised liposomes prepared from new cancerostatic alkylphospholipid BBA 1414:238–48

Zheng J, Ito Y, Imanishi Y (1994) Cell growth on immobilized cell-growth factor: 10. Insulin and polyallylamine co-immobilized materials. Biomaterials 15:963–968. doi:10.1016/0142-9612(94)90076-0